



Published in final edited form as:

Mol Cancer Ther. 2013 September ; 12(9): 1774–1782. doi:10.1158/1535-7163.MCT-12-1023.

Targeted cytolysins synergistically potentiate cytoplasmic delivery of gelonin immunotoxin

Christopher M. Pirie^{1,3}, David V. Liu², and K. Dane Wittrup^{1,2,3}

¹Department of Biological Engineering, Massachusetts Institute of Technology, 77 Massachusetts Avenue, Cambridge, Massachusetts, 02142 USA

²Department of Chemical Engineering, Massachusetts Institute of Technology, 77 Massachusetts Avenue, Cambridge, Massachusetts, 02142 USA

³Koch Institute for Integrative Cancer Research, Massachusetts Institute of Technology, 77 Massachusetts Avenue, Cambridge, Massachusetts, 02142 USA

Abstract

Targeted endocytic uptake is a first step towards tissue-specific cytoplasmic macromolecular delivery; however inefficient escape from the endolysosomal compartment makes this generally impractical at present. We report here a targeted cytolysin approach that dramatically potentiates endosomal release of an independently-targeted potent gelonin immunotoxin. Fibronectin domains engineered for affinity to epidermal growth factor receptor or carcinoembryonic antigen were fused to the plant toxin gelonin or bacterial pore-forming cytolysins. These fusion proteins display synergistic activity in both antigen-specific cytotoxicity *in vitro*, enhancing potency by several orders of magnitude, and in tumor growth inhibition *in vivo*. In addition, the number of internalized gelonin molecules required to induce apoptosis is reduced from $\sim 5 \times 10^6$ to $< 10^3$. Targeted potentiation shows promise for enhancing cytoplasmic delivery of other macromolecular payloads, such as DNA, siRNA, and miRNA.

Keywords

Intracellular delivery; fibronectin; gelonin; epidermal growth factor receptor; carcinoembryonic antigen

Introduction

For decades researchers have pursued a means by which to deliver therapeutic macromolecules such as DNA, RNA, and proteins to the cytoplasm of cells in order to affect intracellular targets, with endosomal escape as the common rate-limiting step (1). Within the fields of gene therapy and RNA interference, the challenge of targeted intracellular delivery is well appreciated (2,3); the same is true for protein therapeutics (4,5). The delivery of

Corresponding Author: K. Dane Wittrup, Massachusetts Institute of Technology, Building 76-261, 77 Massachusetts Avenue, Cambridge, MA 02139, wittrup@mit.edu, Telephone: (617) 253-4578, Fax: (617) 452-3293.

Conflict of Interest: The authors report no conflicts of interest

protein antigens to the intracellular compartment of antigen presenting cells is also enhanced by various mechanisms of endosomal disruption (6,7). Despite measured successes, there remains a critical unmet need for an effective, targeted cytoplasmic delivery approach for macromolecular payloads.

Immunotoxins are a class of proteins that require access to the cytoplasm for their activity. Early developers of immunotoxins diverged in their use of various types of toxins, generally working with either Type I or Type II ribosome inactivating proteins (8). Type II toxins such as diphtheria toxin, ricin, or pseudomonas exotoxin incorporate their own evolved translocation domains or other components that facilitate endosomal escape (9–11). Type I toxins lack similar escape mechanisms, therefore researchers working with Type I toxins have investigated various small molecule and protein based methods for enhancing translocation into the cytoplasm (12–17). These untargeted endosomolytic potentiators lacked specificity and as a result *in vivo* efficacy was typically limited by toxicity.

The bacterium *Listeria monocytogenes* produces listeriolysin O (LLO), a 60kDa cytolysin protein, as a tool for escape from phagosomes in macrophages. Unlike other cytolysins, LLO is preferentially active within the lysosomal compartment. Once the bacterium and protein are released into the cytoplasm, LLO is inactivated through a variety of mechanisms (18), the most important of which is its pH sensitivity (19). LLO and other cytolysins have been used previously as untargeted reagents for the *in vitro* uptake of macromolecules including DNA and proteins (20–24), however untargeted potentiation of this type would not be feasible for *in vivo* application. LLO has also been explored as the cytotoxic component of an immunotoxin (25). Homologs in the cholesterol-dependent cytolysins family (26) include perfringolysin O (PFO) and streptolysin O. Based on our previous findings with Fn3-gelonin immunotoxins and the cytolysin mechanism of action, we hypothesized that targeting LLO or PFO to endocytosed surface antigens would potentiate Type I immunotoxins through enhanced intracellular delivery.

We previously designed a set of immunotoxins based on engineered binding affinity variants of the 10th Type III human fibronectin (Fn3) domain which target either the carcinoembryonic antigen (CEA) or the epidermal growth factor receptor (EGFR) (two canonical tumor-associated antigens) fused to recombinant, plant Type I ribosome inactivating protein gelonin (rGel) (27). These immunotoxins show enhanced, antigen-dependent cytotoxicity towards antigen over-expressing cells. However, they were impotent against lower-expressing cell lines, leading us to investigate and quantify the endosomal escape efficiency of the immunotoxins (27). Previous work in this field (28,29) indicates that only a single immunotoxin molecule may be required to reach the cytoplasm in order to induce apoptosis, yet we found that ~5 million immunotoxin molecules had to be endocytosed to reach this cytoplasmic threshold. Consequently, improved endosomal escape provides an avenue for a potentially greater than million-fold improvement in gelonin immunotoxin potency.

Using the same engineered Fn3s incorporated in our gelonin immunotoxins, we created targeted fusion proteins with LLO and PFO. When combined with gelonin immunotoxins in cell treatments, these targeted cytolysins exhibited potentiating activity, decreasing the IC₅₀

values for our immunotoxins by several orders of magnitude. Potentiation was observed when the two agents were targeted to the same antigen competitively, when targeted to different antigens known to colocalize, and even when targeted to cells expressing low levels of antigens. We further tested the ability of fusions to potentiate immunotoxin activity when the two agents were applied to cells at different times and quantified the reduction in the intracellular barrier to delivery. This was consistent with the improvement in cytotoxicity demonstrating that the observed synergistic effects are the result of membrane destabilization or pore-formation by the cytolysins leading to cytoplasmic release of immunotoxin.

This approach to antigen-specific intracellular delivery using two independently-targeted molecules, *in trans*, is a departure from traditional methods in which the membrane disruptive agent and the macromolecular payload are physically connected. Two different agents targeting the same cell bind to surface antigen and are internalized, becoming colocalized within the same endosomal compartment where the potentiating agent facilitates the release of the macromolecular payload (Fig. 1). The combination of gelonin immunotoxin and cytolysin potentiators are tolerated *in vivo*, and their combination displays synergistic inhibition of tumor growth.

Materials and Methods

Reagents and cell lines

Four different established human cancer cell lines were utilized. All four parental strains were originally obtained from American Type Culture Collection and were authenticated prior to initiation of the described experiments using PromoKine Mycoplasma Test Kits (PromoCell, Heidelberg, Germany). HT-1080 is a human fibrosarcoma cell line negative for CEA. HT-1080(CEA) is a transfected variant of HT-1080 which expresses CEA at high levels ($\sim 2 \times 10^6$ copies/cell) on its surface through the pIRES-CEA plasmid, which is maintained under selective pressure from geneticin. Both HT-1080 and HT-1080(CEA) also express $\sim 1 \times 10^5$ copies of EGFR. A431 is a human epidermoid carcinoma cell line that highly expresses EGFR ($\sim 3 \times 10^6$ copies/cell) but not CEA. HT-29 is a human colorectal carcinoma cell line that expresses lower levels of both CEA and EGFR ($\sim 1 \times 10^5$ copies/cell).

Colocalization microscopy

1×10^5 HT-29 cells were cultured on MatTek dishes with 0.13mm coverslip bottoms in 200 μ L of growth media to which Alexa584-sm3E anti-CEA single-chain antibody variable fragment (7 μ M, DOL 1.85) and Alexa488-225 anti-EGFR antibody (5 μ M, DOL 6) were added with final concentrations of 11.7 nM and 33 nM, respectively. The cells were maintained in this solution under standard culture conditions (37 °C, 5% CO₂) for 15 hours, after which the cells were washed three times with PBS and returned to growth media for 30 minutes before imaging. Cells were serum starved prior to treatment.

Calculation of synergy metrics

Synergy between gelonin immunotoxins and targeted cytolytins *in vitro* was quantified using designed cytotoxicity co-titrations to calculate combination index and cumulative data to calculate synergy assessment factor. The CI metric was first used to determine the synergistic effects of mutually exclusive and mutually non-exclusive enzyme inhibitors by Chou and Talalay (30,31). SAF is a more recent treatment of synergistic effects which was inspired by CI and the Bliss independence criterion (32). It was first put forth by Yan *et al.* as it pertained to synergy within signaling networks (33) and is equivalent to the fractional product equation described by Webb (34). For CI calculations we simultaneously titrated immunotoxins and used 0.9 fraction affected as the analysis point.

$$\frac{[IT]}{IT_{90}} + \frac{[P]}{P_{90}} + \frac{[IT] \times [P]}{(IT, P)_{90}}$$

Alternatively, when using SAF we chose to calculate the metric for all titrations and data points then averaged for cell line or immunotoxin/potentiator of interest.

$$F_A(IT, P) - F_A(IT) \times F_A(P)$$

Quantitative internalization

Cell lines were incubated with immunotoxins directly labeled with AlexaFluor 488 and unlabeled Fn3-cytolysin. At each time point, cells were washed with PBS and incubated for 30 minutes with quenching rabbit anti-AlexaFluor 488 antibody (Invitrogen). Cells were scraped from the wells, washed with PBS, and analyzed for internal fluorescent signal. Quantum Simply Cellular anti-Mouse IgG beads (Bangs Laboratories, Fishers, IN) with different quantified binding capacities were incubated with AlexaFluor 488 labeled mouse IgG for 30 minutes, washed with PBS, then measured for fluorescence. The number of fluorescent molecules per protein on both immunotoxins and mouse IgG was determined using absorbance measurements at 280 and 494 nm. Bead fluorescence measurements were used to generate a standard curve for fluorescence signal per fluorophore. Immunotoxin internalization data were quantified by mapping fluorescence signal to the bead fit, converting signal to fluorescent molecules and then translating into immunotoxin molecules using the labeling ratio.

Xenograft microscopy

Mice with established HT-29 xenograft tumors were treated with PBS or therapeutic combination and their tumors excised and frozen before histology and staining. To examine immunotoxin and potentiator tumor colocalization we labeled C7rGel with AlexaFluor-594 and E6PFO with AlexaFluor-488 then injected half-maximal doses (6 mg/kg C7rGel and 0.1 mg/kg E6PFO) at t = 0 hrs and 8 hrs, respectively. Microtome sections were fixed in acetone to reduce loss of signal and stained with DAPI to visualize nuclei. To examine induction of apoptosis tumors from PBS and combination treated mice were excised, frozen, sectioned,

and then stained with DAPI, rat anti-mouse CD31 (Becton Dickinson, Billerica, MA), and rabbit anti-cleaved caspase-3 (Cell Signaling Technology, Danvers, MA) followed by chicken anti-rat AlexaFluor-594 and goat anti-rabbit AlexaFluor-488. Imaging of both sample sets was conducted on an Applied Precision DeltaVision Spectris Imaging System setup for confocal fluorescence microscopy.

Tumor xenograft growth inhibition

Mice received subcutaneous injections of 3×10^6 HT-29 cells in the right flank on day 0. Digital caliper measurements of tumor volume began on day 5 and were made every second day, for the duration of the study. On day 7 measurements were used to divide mice to treatment groups so as to balance the average tumor volume for each group. Four groups of three mice were used: PBS/PBS, C7rGel/PBS, PBS/E6PFO, and C7rGel/E6PFO as primary/secondary respectively. Treatments were given on day 7 and 11 with 3 hour and 6 hour separations between primary retro-orbital injection and secondary intraperitoneal injection.

Statistical analysis

For binding affinity, cytotoxicity, hemolysis, and plasma clearance data averages were plotted with standard deviation error bars as calculated from triplicate measurements. *in vitro* potentiation affects were analyzed statistically using the CI and SAF methods described above. *in vivo* xenograft growth inhibition data were analyzed statistically using the method of repeated measures analysis of variance (one-way) and p values < 0.1 are reported.

Results and Discussion

The two agent approach was designed to enable independent targeting of a therapeutic macromolecule and a potentiator to distinct antigen targets. Many cell surface antigens, including EGFR and CEA here, have been shown to colocalize (35) and most internalization pathways converge in early endosomes (36).

EGFR and CEA intracellular colocalization

HT-29 cells express approximately 1×10^5 copies each of EGFR and CEA on their surface. These cells were treated with fluorescently labeled anti-EGFR IgG and anti-CEA scFv. Subsequent microscopy images show that both antigens were internalized and compartmentalized with punctate staining (Fig. 2). Further, merged images from the two fluorescent channels indicate extensive colocalization. Colocalization was measured using image analysis software and found to have a Pearson's correlation coefficient of 0.76 (37).

Cytolysin immunotoxin synthesis and *in vitro* characteristics

Novel cytolysin fusion proteins of the Fn3-LLO and Fn3-PFO types were designed with targeting to EGFR and CEA (Supplementary Methods S1). Fusions were derived from Fn3 clones E626 (E6) and C743 (C7), which bind to EGFR and CEA with K_d affinities of 260 pM and 1.8 nM, respectively. The fusions were expressed in *E. coli* at ~ 1.5 mg/L for Fn3LLO and ~ 100 mg/L for Fn3PFO (Supplementary Methods S2). Fn3-LLO variants were assayed for antigen affinity as described by Pirie *et al.* (27), while Fn3-PFO fusions were

titrated on yeast or magnetic beads to eliminate the effects of PFO binding to cholesterol (Supplementary Methods S3). Non-linear regression fitting identified K_d 's of 5.0 nM for E6LLO, 4.0 nM for C7LLO, 4.1 nM for E6PFO and 4.1 nM for C7PFO (Supplementary Fig. S1A).

Independent cytotoxicity of all four fusions was tested by titration on antigen positive and antigen negative cell lines (Supplementary Methods S4). Concentration-response curves with variable slopes fitted to the data yielded IC_{50} values that correlated inversely with antigen expression level (Supplementary Fig. S1B). These data show that targeted LLO and PFO fusions do indeed possess inherent cytotoxicity (25).

The hemolysis assay is a commonly used tool for the characterization of bacterial cholesterol dependent cytolysins and other membrane disruptive materials (Supplementary Methods S5). Fn3-cytolysin fusions' ability to disrupt red blood cells at either physiological or endosomal pH is an indicator of non-specific toxicity or activity, respectively. We were particularly interested in assessing hemolysis because of previous work that suggested very low toxicity limits ($LD_{50} = 0.8 \mu\text{g}$) of LLO *in vivo* (19). At pH 7, the EC_{50} for membrane disruption by E6LLO was ~ 500 nM, while at pH 5 it was ~ 3 nM. For E6PFO, the EC_{50} 's at pH 7 and 5 were ~ 25 pM and ~ 4 pM, respectively (Supplementary Fig. S2). These *in vitro* data support our finding that PFO fusions are more toxic *in vivo* and are consistent with work by Jones and Portnoy that queried LLO and PFO hemolytic characteristics (38).

Potentiated immunotoxin cytotoxicity *in vitro*

Two previously described immunotoxins targeting EGFR and CEA (E4rGel and C7rGel (27)) were tested for potentiation by targeted cytolysins. These immunotoxins have IC_{50} values of approximately 30 nM for E4rGel and 5 nM for C7rGel on cell lines expressing high levels ($>1 \times 10^6$ copies per cell) of antigen. However, on HT-29 cells, which express lower levels of antigen, the immunotoxins appear no more potent than untargeted rGel toxin, with IC_{50} values of $\sim 1 \mu\text{M}$. Remarkably, when immunotoxins are titrated in the presence of non-toxic levels of Fn3-targeted cytolysins, the gelonin immunotoxin potency is increased by several orders of magnitude. On cells expressing high levels of antigen, the IC_{50} of E4rGel is decreased from 30 nM to 40 pM and that of C7rGel is potentiated from 600 pM to < 30 pM (Supplementary Fig. S3). Perhaps most importantly, cytotoxicity on HT-29 cells of the otherwise ineffective immunotoxins was potentiated to an equivalent degree where the IC_{50} 's shifted from 1 μM to 1 nM (Fig. 3A). This shift was observed with non-competitively co-targeted immunotoxin and potentiator, components targeted to different antigens, and antigen-negative (HT-1080) cells for which the IC_{50} value for C7rGel was reduced from 1 μM to 30 nM

Observed synergy between gelonin and cytolysin immunotoxins was quantified using two different metrics: combination index (CI) and synergy assessment factor (SAF) (30,31,33). CI values characterize an interaction as antagonistic when > 1 , additive when $= 1$, and synergistic when < 1 . Similarly, SAF will be > 0 when antagonistic, $= 0$ when a combination is additive, and < 0 when synergistic. For example, when HT-29 cells were treated with C7rGel, potentiation by E6LLO resulted in a CI_{90} (at 90% efficacy) of 0.03 and a SAF of -0.58 and for E6PFO $CI_{90} = 0.11$ and SAF = -0.32. CI_{90} values less than 1 and negative SAF

values, indicative of strong synergy, were observed across all combinations of cytolysin fusions and gelonin immunotoxins on all tested cell lines. The strength of synergy observed using either metric tended to show an inverse correlation with the independent potency of the gelonin immunotoxin or potentiator on the cell line in question.

Internalized cytotoxicity and reduction of the intracellular barrier

Previously we showed that there is an intracellular barrier to immunotoxin potency which leads to a requirement for $\sim 5 \times 10^6$ endocytosed toxin molecules before a cell undergoes apoptosis (27), across all cell types tested, antigens targeted, and binding affinities measured. The same technique described therein was used here to characterize the intracellular barrier in the presence of potentiator. We observed the expected increase in the number of anti-CEA immunotoxins internalized by HT-29 cells with increasing treatment concentration and incubation time (Supplementary Fig. S4A). However, loss of viability is observed in treatment matched cells while the number of immunotoxins internalized is considerably less than would be necessary to induce cytotoxicity in the absence of potentiator (Supplementary Fig. S4B).

When we combine data from internalization and cytotoxicity measurements we obtain potency curves that show the number of internalized molecules inducing 50% growth inhibition (TN_{50}) is $< 10^3$ molecules, indicating a several order of magnitude drop in the delivery barrier due to the presence of potentiator (Supplementary Fig. S4C). In fact, we are unable to directly ascertain the true TN_{50} in the presence of potentiator because the fluorescent signal from so few molecules is indiscernible from autofluorescence of the cells. Internalized cytotoxicity measurements for anti-CEA immunotoxins on HT-1080, HT-1080(CEA), and HT-29 cells in the presence of CEA or EGFR potentiator plotted alongside the curve-fit for unpotentiated TN_{50} from our previous work (27) illustrate the magnitude of the enhancement of intracellular delivery due to potentiator (Fig. 3B). Somewhat surprisingly, cytoplasmic delivery of immunotoxin was also enhanced in antigen-negative cells, suggesting that potentiation is achieved even at low pinocytic levels of immunotoxin internalization.

By validating the hypothesized mechanism of potentiation (reduction of the intracellular barrier) using the previously developed internalization/cytotoxicity assay, the broader applicability of the targeted *in trans* intracellular macromolecular delivery approach is supported. Assuming that the molecular mechanism of cytolysin action is that of pore formation (26), these results suggest that other macromolecular payloads with physical characteristics similar to that of rGel should be able to experience increased access to the cytoplasm. Recently, we have conducted follow-on studies which suggest that similar outcomes will be observed for targeted DNA. Therefore it is reasonable to expect that other targeted macromolecules, such as targeted siRNA or miRNA, will be enhanced by concomitant treatment with Fn3-cytolysin fusions.

Delayed exposure cytotoxicity

To reduce simultaneous non-specific uptake of both active agents by antigen-negative cells *in vivo*, we developed a system in which the two agents might be dosed independently at

different times. This degree of freedom is available only by using the two agents separately, in trans. The feasibility of this approach was tested *in vitro* by treating cells for a fixed period of time with growth media containing one agent, then removing it and replacing it with new media containing the appropriate second agent. A431 cells were treated with anti-EGFR immunotoxin for 12 hours and then non-competitive anti-EGFR potentiator for 24 hours with potentiator exposure delayed 0, 12, 24, or 48 hours. Similarly, HT-29 cells were exposed to differentially targeted immunotoxin (CEA) and potentiator (EGFR) at order of magnitude higher concentrations, to compensate for reduced antigen expression, resulting in stronger but consistent results. A ~5-fold increase in cell viability was observed as exposure delay time was increased (Fig. 4). Treatment concentrations for each agent were non-toxic when exposed independently, and synergistic effects were apparent regardless of the order in which the agents were incubated. These data indicate that immunotoxin dosed in the first phase persists either at the cell surface or intracellularly for 12-48 hours in sufficient amounts to induce apoptosis when subsequently dosed with targeted cytolysin. This allows for considerable temporal separation of dosing for the two agents (immunotoxin and targeted potentiator) when administered independently *in vivo*.

Independent *in vivo* dosing and clearance of gelonin or cytolysin immunotoxins

Toxicity of these agents in nude mice was assessed by the “3+3 dosing method” (39) (Supplementary Methods S6) with increasing amounts of either gelonin immunotoxin or targeted cytolysin until dose limiting toxicity was observed. For CEA-targeted C7rGel no substantial toxicity was observed up to doses of 16 mg/kg while for E6LLO and E6PFO dose limiting toxicities were reached above 0.6 and 0.2 mg/kg respectively (Supplementary Table S1). Interestingly, these maximum tolerated doses correlate roughly with non-specific cytotoxicity IC₅₀ values on antigen-negative cells for each fusion observed *in vitro* when converted based on assumed volumes for serum or intraperitoneal fluid. Maximum tolerated doses were used for all subsequent experiments.

To direct the choice of dose-separation time delay the plasma half-lives of these agents were evaluated. Bi-exponential fitting of protein clearance data from retro-orbital injections yielded alpha-phase half-lives and beta-phase half-lives of 30 minutes and 12.2 hours for C7rGel, 124 minutes and 11.5 hours for E6LLO, and 34 minutes and 13.3 hours for E6PFO. Tri-exponential fitting of data from intraperitoneal injections of E6PFO revealed a plasma absorption half-time of 65 minutes. Examples of clearance data and curve fitting results are provided (Supplementary Fig. S5). While it is possible to target both components (*i.e.*, a therapeutic agent, such as Fn3-rGel, and a potentiating agent, such as Fn3-LLO or Fn3-PFO) to the same cell-surface molecule (Fig. 3A), independent targeting of two different antigens should be preferred since it can confer additional targeting specificity and reduced toxicity *in vivo*.

Combination treatment of murine xenografts

The toxicity of dual agent treatment was assessed initially with sequential retro-orbital injection of both agents where C7rGel was injected first and E6LLO or E6PFO was injected second. The time delay between immunotoxin and potentiator doses was decreased linearly, again using the “3+3 method”, until dose-separation limiting toxicity was observed. Results

indicated that when using this route of administration E6LLO could be dosed no sooner than 12 hours after C7rGel injection, and the minimum delay with E6PFO was 24 hours (Supplementary Table S2). We also investigated the possibility of intraperitoneal injection of targeted cytolytins, secondary to retro-orbital dosing of C7rGel. Injection of a bolus into the peritoneal cavity provides a more gradual uptake into the plasma while residual gelonin immunotoxins from a previously administered dose remain in the tumor (40). When administering C7rGel by retro-orbital injection followed by intraperitoneal injection of targeted cytolytin we found that E6LLO and E6PFO doses could follow as little as 6 hours and 3 hours after, respectively (Supplementary Table S2).

Once the maximum tolerated dose and minimum dose separation time were determined, a tumor xenograft model was used to assess *in vivo* efficacy of combination treatment. When mice were given both therapeutic agents in succession, they were found to colocalize in the tumor interstitium (Fig. 5A) and their combined presence in the tumor induced apoptosis not observed in PBS treated tumors (Fig. 5B). To investigate tumor growth inhibition, nude mice bearing developed HT-29 colorectal carcinoma xenografts were dosed with either phosphate buffered saline (PBS), C7rGel & PBS, PBS & E6PFO, or C7rGel & E6PFO at days 7 and 9 post tumor injection. Individual therapeutic treatments were unable to control tumor growth, but the combination treatment resulted in statistically significant ($p = 0.053$) inhibition of tumor progression (Fig. 6). It should be noted that in the combination treatment group, one of the mice had to be euthanized due to acute toxicity. This combination treatment toxicity as well as the single dose cytolytin toxicity measured in these experiments with immune compromised mice does not capture the likely immunogenic limitations (41) of these fusion proteins in their current form which could limit repeated dosing. Nevertheless, these *in vivo* studies show the potential of this combination system as an effective anti-cancer therapy. The selected dosing regimen was able to control xenograft tumor growth with just two rounds of treatment.

Conclusions

Combined treatment systems like the one described herein will likely require optimization to reduce residual non-specific toxicities or immunogenicity in order to improve efficacy. Specifically, the particular forms of the binding and cytolytin components of the fusion protein may need to be engineered to adjust affinity or endosomal/membrane disruption. One likely cause of cytotoxicity towards antigen-negative cells and dose-limiting toxicities *in vivo* is the non-specific membrane interaction of the cytolytin domains. Direct protein engineering of the cytolytins themselves or fusion incorporation of binding domains shielding the membrane interaction residues might reduce such toxicities without attenuating potentiation effects. Moreover, an antigenic epitope remove procedure similar to that described by Onda *et al.* (42) would need to be applied for repeated dosing to be enabled. In each formulation, the dosing of the potentiating fusion protein and the cytoplasm-active agent will most likely have to be determined on an empirical basis with respect to scale, timing, and frequency. Following optimization of cytolytins and fusion constructs, more thorough *in vivo* studies (including model systems capable of immune response) will need to be performed before the *in trans* therapeutic approach can be advanced as a clinical strategy.

Recognizing that targeted intracellular delivery is a critical component of the efficacy of numerous therapeutic agents (3), including immunotoxins (27), we set out to develop a new independent targeting method. Our studies are the first to use cytolysins as targeted *in trans* potentiating endosomolytic agents together with an independently targeted macromolecular payload. One benefit of this approach is that targeting two independent antigens can improve *in vivo* tissue specificity. Additionally, when two agents are delivered *in trans*, they can be dosed at well-separated times, further reducing toxicity in nontargeted tissues. Delivery *in trans* is also useful when the two agents have differing toxicity limits. The results here indicate that this independently-targeted two agent approach is a promising tool for targeted intracellular delivery of macromolecular therapeutics.

Supplementary Material

Refer to Web version on PubMed Central for supplementary material.

Acknowledgments

The authors acknowledge Dr. Michael Rosenblum for insightful discussions and input. We thank Dr. Ryan Lim for assistance with fermentation protein synthesis and Dr. Jamie Spangler for assistance with *in vitro* microscopy. For histology support we thank John Rhoden. The Koch Institute Swanson Biotechnology Center provided DNA sequencing, microscopy, and histology resources.

Financial Support: This work was supported by National Science Foundation Grant U54CA119349 and National Institutes of Health Grants CA101830 and AI065824 to KDW. C.M.P. was supported in part by a National Science Foundation Graduate Research Fellowship.

References

1. Shim MS, Kwon YJ. Efficient and targeted delivery of siRNA *in vivo*. *FEBS J.* 2010 Dec. 277:4814–27. [PubMed: 21078116]
2. Lares MR, Rossi JJ, Ouellet DL. RNAi and small interfering RNAs in human disease therapeutic applications. *Trends Biotechnol.* 2010 Nov.28:570–9. [PubMed: 20833440]
3. Varkouhi AK, Scholte M, Storm G, Haisma HJ. Endosomal escape pathways for delivery of biologicals. *J Control Release.* 2011 May 10.151:220–8. [PubMed: 21078351]
4. Nishikawa M, Hashida M, Takakura Y. Catalase delivery for inhibiting ROS-mediated tissue injury and tumor metastasis. *Adv Drug Deliv Rev.* 2009 Apr 28.61:319–26. [PubMed: 19385054]
5. Zhao M, Biswas A, Hu B, Joo KI, Wang P, Gu Z, et al. Redox-responsive nanocapsules for intracellular protein delivery. *Biomaterials.* 2011 Aug.32:5223–30. [PubMed: 21514660]
6. Paterson Y, Guirnalda PD, Wood LM. Listeria and Salmonella bacterial vectors of tumor-associated antigens for cancer immunotherapy. *Semin Immunol.* 2010 Jun.22:183–9. [PubMed: 20299242]
7. Foster S, Duvall CL, Crownover EF, Hoffman AS, Stayton PS. Intracellular delivery of a protein antigen with an endosomal-releasing polymer enhances CD8 T-cell production and prophylactic vaccine efficacy. *Bioconjug Chem.* 2010 Dec 15.21:2205–12. [PubMed: 21043513]
8. Stirpe F, Barbieri L. Ribosome-inactivating proteins up to date. *FEBS Lett.* 1986 Jan 20.195:1–8. [PubMed: 3510899]
9. Kelley VE, Bacha P, Pankewycz O, Nichols JC, Murphy JR, Strom TB. Interleukin 2-diphtheria toxin fusion protein can abolish cell-mediated immunity *in vivo*. *Proc Natl Acad Sci U S A.* 1988 Jun.85:3980–4. [PubMed: 3131768]
10. Bjorn MJ, Groetsema G, Scalapino L. Antibody-Pseudomonas exotoxin A conjugates cytotoxic to human breast cancer cells *in vitro*. *Cancer Res.* 1986 Jul.46:3262–7. [PubMed: 3011243]
11. Seon BK. Specific killing of human T-leukemia cells by immunotoxins prepared with ricin A chain and monoclonal anti-human T-cell leukemia antibodies. *Cancer Res.* 1984 Jan.44:259–64. [PubMed: 6606488]

12. Wu M. Enhancement of immunotoxin activity using chemical and biological reagents. *Br J Cancer*. 1997; 75:1347–55. [PubMed: 9155057]
13. Wu YN, Gadina M, Tao-Cheng JH, Youle RJ. Retinoic acid disrupts the Golgi apparatus and increases the cytosolic routing of specific protein toxins. *J Cell Biol*. 1994 May.125:743–53. [PubMed: 8188744]
14. Vitetta ES, Cushley W, Uhr JW. Synergy of ricin A chain-containing immunotoxins and ricin B chain-containing immunotoxins in in vitro killing of neoplastic human B cells. *Proc Natl Acad Sci U S A*. 1983 Oct.80:6332–5. [PubMed: 6578512]
15. Greenfield L, Johnson VG, Youle RJ. Mutations in diphtheria toxin separate binding from entry and amplify immunotoxin selectivity. *Science*. 1987 Oct 23.238:536–9. [PubMed: 3498987]
16. Goldmacher VS, Blättler WA, Lambert JM, McIntyre G, Stewart J. Cytotoxicity of gelonin conjugated to targeting molecules: effects of weak amines, monensin, adenovirus, and adenoviral capsid proteins penton, hexon, and fiber. *Mol Pharmacol*. 1989 Nov.36:818–22. [PubMed: 2531272]
17. FitzGerald DJ, Trowbridge IS, Pastan I, Willingham MC. Enhancement of toxicity of antitransferrin receptor antibody-Pseudomonas exotoxin conjugates by adenovirus. *Proc Natl Acad Sci U S A*. 1983 Jul.80:4134–8. [PubMed: 6306663]
18. Schnupf P, Portnoy DA. Listeriolysin O: a phagosome-specific lysin. *Microbes Infect*. 2007 Aug. 9:1176–87. [PubMed: 17720603]
19. Geoffroy C, Gaillard JL, Alouf JE, Berche P. Purification, characterization, and toxicity of the sulfhydryl-activated hemolysin listeriolysin O from *Listeria monocytogenes*. *Infect Immun*. 1987 Jul.55:1641–6. [PubMed: 3110067]
20. Sun X, Provoda C, Lee KD. Enhanced in vivo gene expression mediated by listeriolysin O incorporated anionic LPDII: Its utility in cytotoxic T lymphocyte-inducing DNA vaccine. *J Control Release*. 2010 Dec 1.148:219–25. [PubMed: 20620181]
21. Giles RV, Spiller DG, Grzybowski J, Clark RE, Nicklin P, Tidd DM. Selecting optimal oligonucleotide composition for maximal antisense effect following streptolysin O-mediated delivery into human leukaemia cells. *Nucleic Acids Res*. 1998 Apr 1.26:1567–75. [PubMed: 9512525]
22. Walev I, Bhakdi SC, Hofmann F, Djonder N, Valeva A, Aktories K, et al. Delivery of proteins into living cells by reversible membrane permeabilization with streptolysin-O. *Proc Natl Acad Sci U S A*. 2001 Mar 13.98:3185–90. [PubMed: 11248053]
23. Provoda CJ, Stier EM, Lee KD. Tumor cell killing enabled by listeriolysin O-liposome-mediated delivery of the protein toxin gelonin. *J Biol Chem*. 2003 Sep 12.278:35102–8. [PubMed: 12832408]
24. Kerr DE, Wu GY, Wu CH, Senter PD. Listeriolysin O potentiates immunotoxin and bleomycin cytotoxicity. *Bioconjug Chem*. 1997 Dec.8:781–4. [PubMed: 9404648]
25. Bergelt S, Frost S, Lilie H. Listeriolysin O as cytotoxic component of an immunotoxin. *Protein Sci*. 2009 Jun.18:1210–20. [PubMed: 19472336]
26. Tweten RK. Cholesterol-dependent cytolysins, a family of versatile pore-forming toxins. *Infect Immun*. 2005 Oct.73:6199–209. [PubMed: 16177291]
27. Pirie CM, Hackel BJ, Rosenblum MG, Wittrup KD. Convergent potency of internalized gelonin immunotoxins across varied cell lines, antigens, and targeting moieties. *J Biol Chem*. 2011 Feb 11.286:4165–72. [PubMed: 21138845]
28. Yamaizumi M, Mekada E, Uchida T, Okada Y. One molecule of diphtheria toxin fragment A introduced into a cell can kill the cell. *Cell*. 1978 Sep.15:245–50. [PubMed: 699044]
29. Yazdi PT, Murphy RM. Quantitative analysis of protein synthesis inhibition by transferrin-toxin conjugates. *Cancer Res*. 1994 Dec 15.54:6387–94. [PubMed: 7987833]
30. Chou TC, Talalay P. Analysis of combined drug effects: a new look at a very old problem. *Trends in Pharmacological Sciences*. 1983; 4:450–4.
31. Chou TC, Talalay P. Quantitative analysis of dose-effect relationships: the combined effects of multiple drugs or enzyme inhibitors. *Adv Enzyme Regul*. 1984; 22:27–55. [PubMed: 6382953]
32. Bliss CI. The Toxicity Of Poisons Applied Jointly1. *Annals of Applied Biology*. 1939 Aug 1.26:585–615.

33. Yan H, Zhang B, Li S, Zhao Q. A formal model for analyzing drug combination effects and its application in TNF- α -induced NF κ B pathway. *BMC Syst Biol.* 2010; 4:50. [PubMed: 20416113]
34. Webb, J. *Enzyme and Metabolic Inhibitors* Internet. New York: Academic Press; 1963. p. 55-79. Available from
35. Xing Y, Smith AM, Agrawal A, Ruan G, Nie S. Molecular profiling of single cancer cells and clinical tissue specimens with semiconductor quantum dots. *Int J Nanomedicine.* 2006; 1:473–81. [PubMed: 17722280]
36. Mayor S, Pagano RE. Pathways of clathrin-independent endocytosis. *Nat Rev Mol Cell Biol.* 2007 Aug; 8:603–12. [PubMed: 17609668]
37. Adler J, Parmryd I. Quantifying colocalization by correlation: the Pearson correlation coefficient is superior to the Mander's overlap coefficient. *Cytometry A.* 2010 Aug; 77(8):733–42. [PubMed: 20653013]
38. Jones S, Portnoy DA. Characterization of *Listeria monocytogenes* pathogenesis in a strain expressing perfringolysin O in place of listeriolysin O. *Infect Immun.* 1994 Dec; 62:5608–13. [PubMed: 7960143]
39. Lin Y, Shih WJ. Statistical Properties of the Traditional Algorithm-based Designs for Phase I Cancer Clinical Trials. *Biostat.* 2001 Jun 1; 2:203–15.
40. Barrett JS, Wagner JG, Fisher SJ, Wahl RL. Effect of intraperitoneal injection volume and antibody protein dose on the pharmacokinetics of intraperitoneally administered IgG2a kappa murine monoclonal antibody in the rat. *Cancer Res.* 1991 Jul 1; 51:3434–44. [PubMed: 1905196]
41. Carrero JA, Vivanco-Cid H, Unanue ER. Listeriolysin o is strongly immunogenic independently of its cytotoxic activity. *PLoS ONE.* 2012; 7:e32310. [PubMed: 22403645]
42. Onda M, Beers R, Xiang L, Lee B, Weldon JE, Kreitman RJ, et al. Recombinant immunotoxin against B-cell malignancies with no immunogenicity in mice by removal of B-cell epitopes. *Proc Natl Acad Sci U S A.* 2011 Apr 5; 108:5742–7. [PubMed: 21436054]

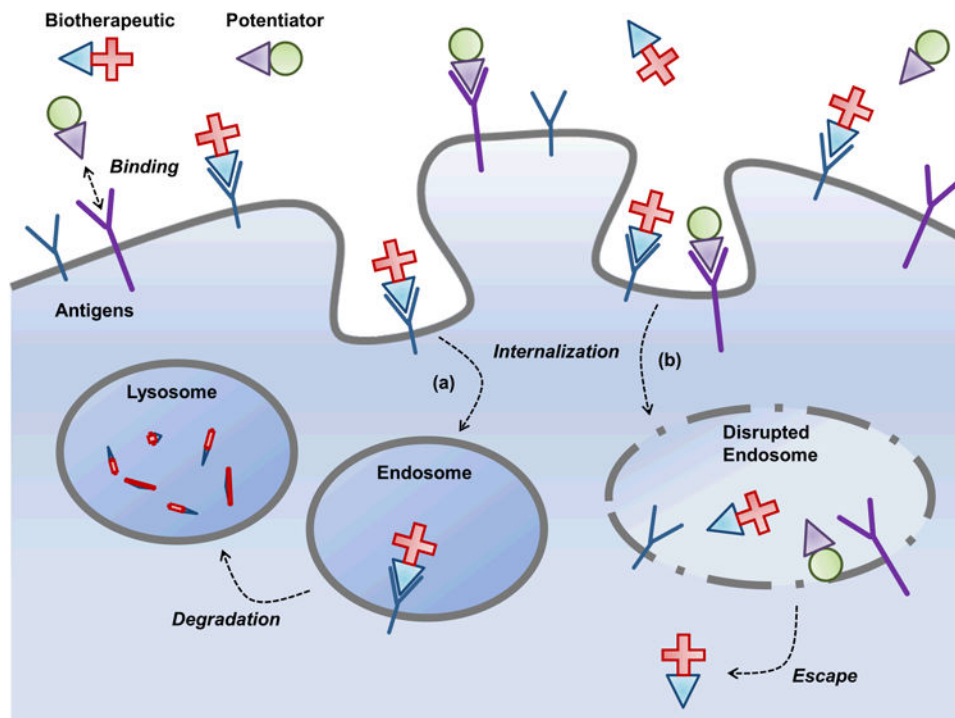


Figure 1.

A two agent intracellular delivery system. The central concept of this work is that independently targeted, membrane disrupting functionality can be delivered to tumor cells via Fn3-cytolysin fusions. Simultaneous targeted delivery of such a Potentiator to tumor cells that internalize by endocytosis an independently targeted Biotherapeutic will potentiate the therapeutic effect by improving escape to the cytoplasm, the site of action. By separating the membrane-crossing and therapeutic components, we are able to dramatically improve specificity and potency. The traditional fate of intracellularly active biotherapeutics (a) leads to degradation in the lysosome, but upon compartmental colocalization of biotherapeutic and potentiator (b), the lysin's membrane disruptive characteristics facilitate therapeutic access the cytoplasm

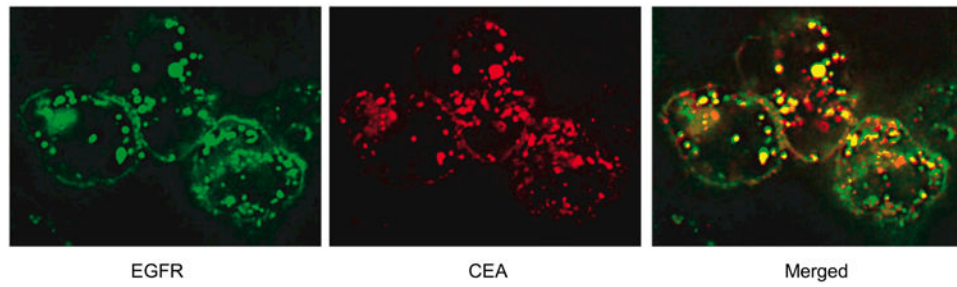


Figure 2. Colocalization of intracellular EGFR and CEA. HT-29 cells that express both EGFR and CEA show that agents targeted to these two receptors will colocalize to a considerable extent to the same intracellular compartments, a necessary condition for the success of the proposed potentiation strategy. An anti-EGFR antibody was conjugated with AlexaFluor-488 and an anti-CEA scFv was conjugated with AlexaFluor-594 before both were used to label HT-29 cells to observe colocalization.

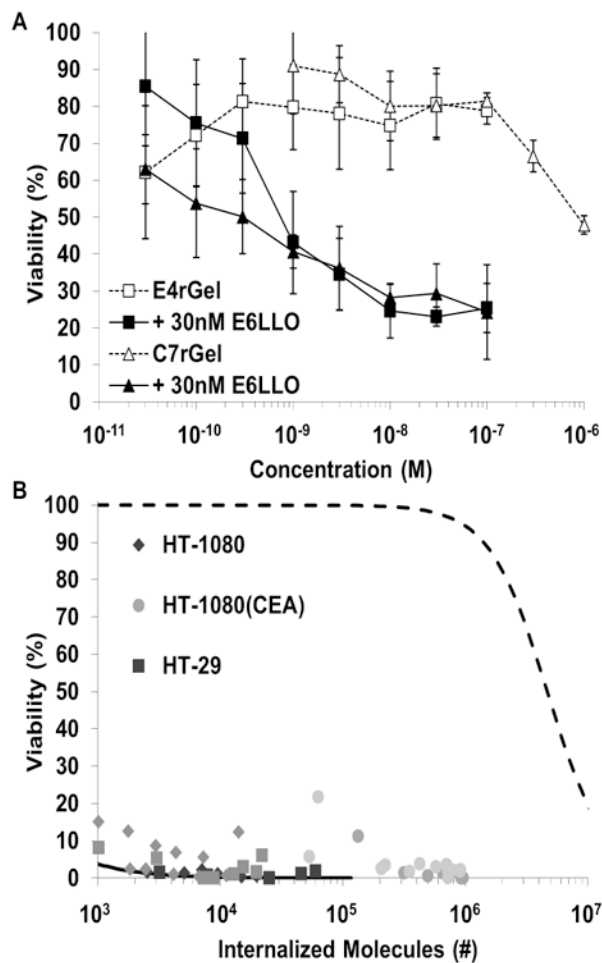


Figure 3. *in vitro* potentiation of immunotoxin activity. Fn3-cytolysins were first tested *in vitro* to show that the fundamental IC₅₀ of Fn3-rGel's could be lowered. (a) HT-29 cells titrated with immunotoxins targeting either EGFR or CEA display no cytotoxicity up to nearly μM concentrations. But in the presence of non-toxic levels of potentiator, these same immunotoxins have IC₅₀'s around 1 nM. (b) Internalized cytotoxicity data from HT-1080, HT-1080(CEA) and HT-29 cells treated with C7rGel and E6LLO are compared to the unpotentiated curve fit (27). In the presence of potentiator, substantially less immunotoxin uptake is required ($< 10^3$ toxin molecules versus 5×10^6) to induce loss of viability.

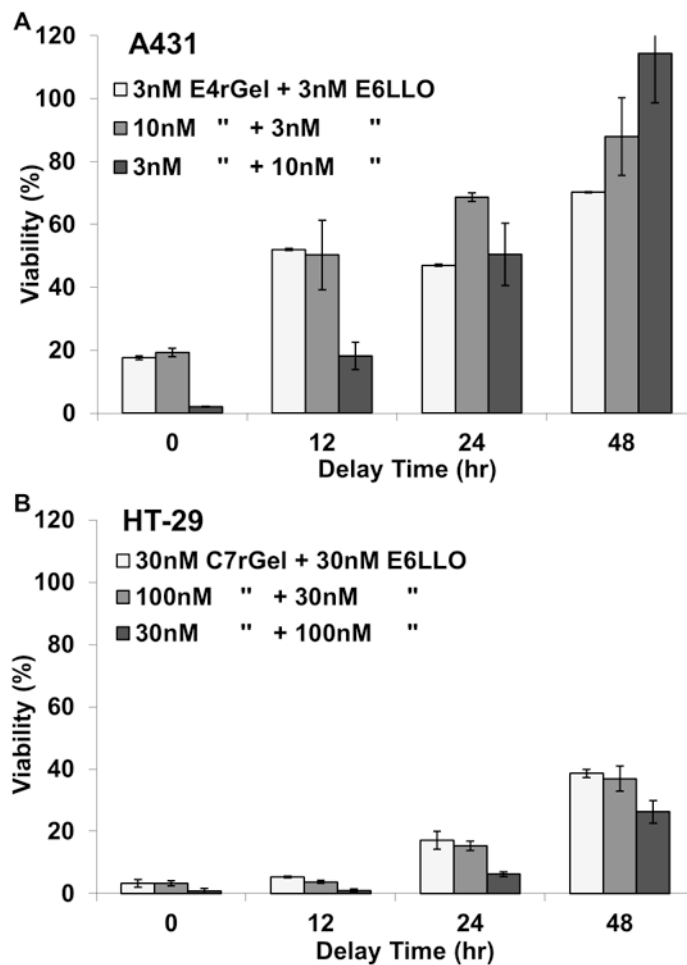


Figure 4.

In these experiments cells were exposed to a concentration of immunotoxin for 12 hours and a concentration of potentiator for 24 hours with potentiator exposure starting at either the same time ($t=0$) or delayed by 12, 24, or 48 hours. **(a)** A431 cells treated with E4rGel immunotoxin and E6LLO potentiator, both non-competitively targeting EGFR. **(b)** HT-29 cells treated with C7rGel immunotoxin targeting CEA and E6LLO potentiator targeting EGFR. We observe that potentiators can be effective even after a 48 hour delay in treatments depending on concentration.

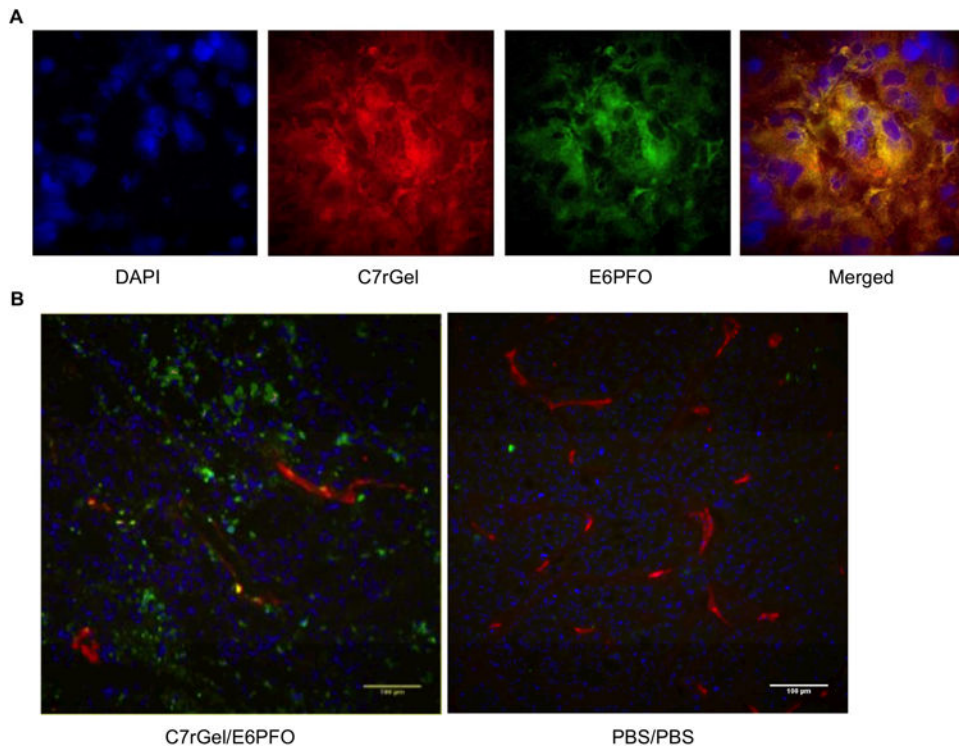


Figure 5. Immunotoxins and targeted cytolytins in tumor xenografts. After establishing maximum tolerated doses and minimum separation times, HT-29 tumor bearing mice were injected with therapeutic combinations of immunotoxin and potentiator or PBS controls. **(a)** Deconvolved images of a labeled combination treated tumor shows accumulation of both therapeutics (C7rGel:red, E6PFO:green) in the tumor interstitium. **(b)** Tumors treated with the drug combination (left) show greater staining for the apoptosis marker cleaved caspase-3 (green) compared to those treated with PBS (right). In both panels cells are identified by nuclear staining with DAPI (blue) and vasculature is labeled with α CD-31 antibody (red).

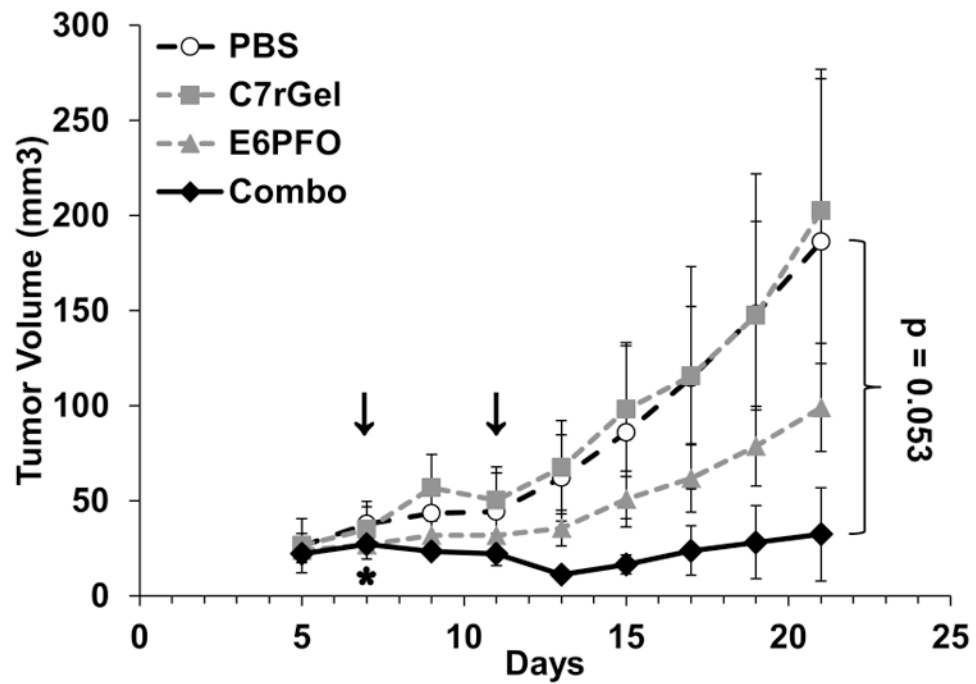


Figure 6. Combination therapy inhibition of xenograft tumor growth. HT-29 tumor xenograft growth is inhibited slightly by independent drug treatments, but only the combination exhibits a significant ($p = 0.053$) delay in tumor growth. Arrows indicate days when doses were administered to all groups. *One mouse in the Combo group was euthanized following day 7 dosing and not used for statistical analysis.